Hindawi
International Journal of Photoenergy
Volume 2018, Article ID 9139683, 11 pages
https://doi.org/10.1155/2018/9139683

Research Article

CFD Analysis and Electrical Efficiency Improvement of a Hybrid PV/T Panel Cooled by Forced Air Circulation

Gökhan Ömeroğlu

Mechanical Engineering Department, Engineering Faculty, Atatürk University, 25300 Erzurum, Turkey

Correspondence should be addressed to Gökhan Ömeroğlu; gomeroglu@atauni.edu.tr

Received 17 August 2017; Accepted 20 February 2018; Published 8 April 2018

Academic Editor: Philippe Poggi

The thermal and electrical efficiency of a custom-designed PV/T panel cooled by forced air circulation was investigated by experimental and computational fluid dynamics (CFD) analysis. Experiments were carried out with four different array configurations, under constant irradiation of 1100 W/m^2 and 3 different air velocities (3.3 m/s, 3.9 m/s, and 4.5 m/s). The heat transfer surface area and forced air circulation are known to positively affect the total heat transfer, and therefore, it is foreseeable that an increased number of fins and higher air velocities will help maintain the electrical efficiency of the panel at higher levels. The main objective of this study is to determine the critical threshold for the abovementioned parameters as well as to show how important parameters, such as fin arrangement and consequent turbulent air flows, are for satisfying the heat removal needs. Highest efficiency was achieved with a 108 pc type 1 arrangement at 12.02% as expected. Nevertheless, while the 108 pc type 2 arrangement could maintain the electrical efficiency at 11.81%, a close level of 11.55% could be obtained with a 54 pc type 2 arrangement. Experimental results are compared with ANSYS Fluent program, and the effect of the number and arrangement of the fins on the efficiency of the panel has been shown.

1. Introduction

A photovoltaic/thermal (PV/T) collector is considered to be a solar collector combined with a photovoltaic module and produces electricity and heat at the same time. Different kinds of solar energy systems are used in various engineering fields [1]. There are mainly two types of PV/T collectors depending on the medium used to collect the thermal energy, air-based and water-based. PV/T air collectors are significantly advantageous than are PV/T water collectors, which require a variety of thermal collection materials depending on PV modules. One of the most important components of a solar energy system is the collector. The various applications of the solar energy collectors have been well recorded [2]. Solar collectors can be used in various areas especially for drying, floor heating, and solar desalination and so on Conventional solar air collectors have inherent disadvantages in lower thermal efficiency. Ekechukwu and Norton [3] conducted experiments to demonstrate a typical 40% to 50% efficiency of the conventional solar air collector. For a PV/T air collector with a ventilated system, the heat losses from PV to air flow are generally not very good, so the losses in the environment are large and the average thermal efficiency is around 10% to 20% [4]. Wijeysundera et al. [5] also investigated the thermal performance of single-glazed and double-glazed multipass solar air heaters. Choudhury et al. [6] found that the single-plated double-pass air heater was the most cost effective compared to the other design. Joshi et al. [7] performed a new optimum efficiency of a hybrid PV/T system. To investigate the performance in New Delhi meteorological conditions, they investigated two types of PV modules (glass-to-plastic and glass-to-glass) and the results show that the overall performance of the hybrid thermal collector with a glass-to-glass PV module is better than with a glass-to-plastic module.

In addition, Choudhury et al. [8] studied theoretical models for single- and double-ended three-pass solar air heaters. Ho et al. [9] studied the improvement of device performance of external recirculating multipass solar air heaters under counter flow conditions. Fudholi et al. [10] stated that they had achieved efficiencies as high as 70% of multipass solar collectors with an increased heat transfer surface.

(a) (b)

Figure 1: (a) PV/T hybrid test setup. (b) Artificial solar radiation and the position of the photovoltaic panel.

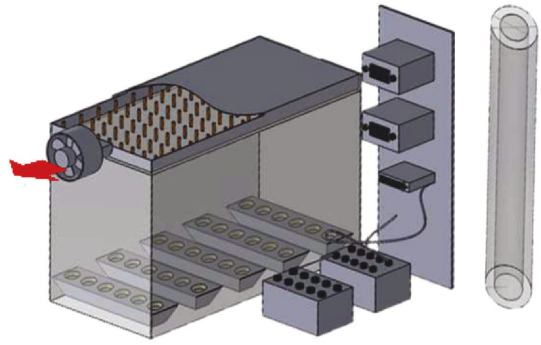

(a) (b)

Figure 2: (a) Schematic view of the experimental setup. (b) Fin geometry.

The different pathways leading to significant improvements in collector efficiency are, for example, corrugated surfaces [11–13], matrix-type absorbers [14], composite honeycomb aggregators [15], box-type absorbers [16], porous media [17], and finned absorbers [18–20].

This study shows that the heat transfer coefficient increases with increasing Reynolds number. The thermal efficiency of the PV module increases with increasing flow rate. In this study, investigating the effect of active cooling with different configurations, such as the fin number, arrangement, and air velocity, on the electrical efficiency of the PV module is aimed. Moreover, a CFD model has been used to validate the results of the experiments. The main objective was to investigate the effects of fin arrangement and subsequent formation of turbulent air rather than the heat transfer surface area (the number of fins in this case) and air velocity on the total heat drawn from the PV panel. As the highest insolation on the earth's surface is 1100 W/m^2, this figure was chosen for the experiments.

The fins used in this study are cheap and easy to manufacture. Besides, on the contrary to other heat transfer elements used in other studies, it is the first time that they are being used in PV/T systems. Another reason to choose them is that they are easy to install and offer a quite low friction loss during the air circulation and hence does not require a high fan power.

2. Material and Methodology

A test setup was designed to investigate the thermal and electrical performance of the PV/T air system. This system was studied in the Renewable Energy Resources Laboratory in Ataturk University. A general view of the experimental setup and a schematic diagram is shown in Figures 1 and 2(a), respectively. A fan with 10 W of power has been employed to feed more air through the control volume in order to create forced convection, and ambient air, used as the working fluid, was sucked through the air duct of the test setup, as shown in Figure 2. The fan is attached to the outlet of the control volume rather than the inlet in order to prevent the fan from heating up the feed air entering the control volume over time.

This experimental study was designed to investigate how temperature affects the efficiency and power output of a PV panel during operation and by using various fin arrays. Polycrystalline solar modules were used in the experiment to generate electricity. The electricity generated by the solar modules is stored in batteries. And the fan was powered by the PV per se, and no external power supply is employed for feeding air. In order to increase the active cooling effect, copper fins, the specifications of which are given in Table 1 and illustrated in Figure 2(b), were fitted in different arrangements as shown in Figure 3. The copper fins were glued with thermal paste onto the back of the PV module, and the air

Table 1: Physical properties of copper cylindrical fins.

Specific weight (kg/dm^3)	Thermal conductivity (W/m·K)	Melting point (°C)	Specific heat capacity (kcal/kg·K)	Resistivity ($\mu\Omega$)	Weight (kg/m)	Outer/inner diameter (mm)	Length (mm)
8.9	336	1065–1085	0.092	1.71	0.70	12/10	50

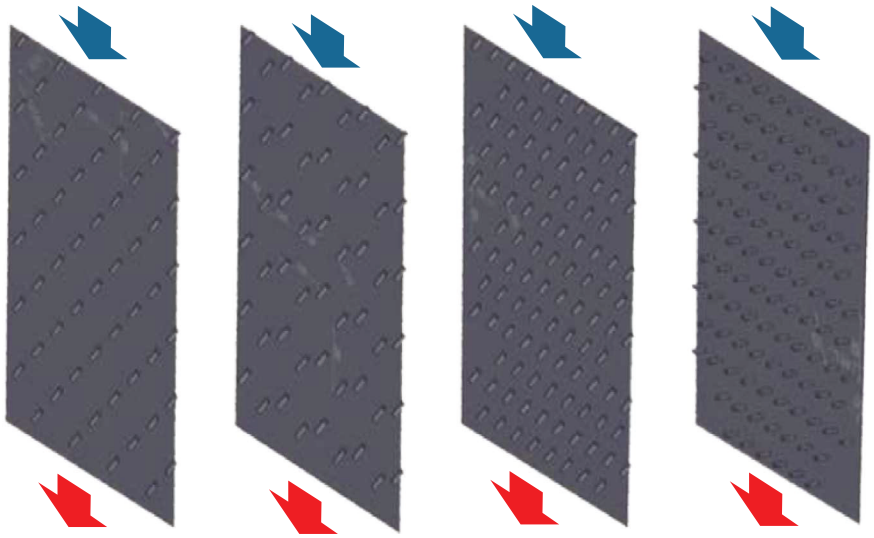

Figure 3: Placement and arrangement of fin configurations.

duct providing air passage was connected to the back of the PV module. The inlet/outlet manifold of the duct uses precision air pressure and velocity gauges to ensure that the air pressure and velocity of the air have been also measured when uniform air flow is being made. Temperature measurements have a crucial role in this experiment and were therefore used to calibrate T-type thermocouples. In this experiment, the PV current, the PV voltage, the temperature of the panels, the air temperatures at the inlet and outlet manifolds, the air velocity, and the solar radiation were measured. Also in this experiment, instead of natural sunlight, artificial solar radiation was used. The panel size is 55 cm wide and 120 cm in length.

The copper fins are attached to the back surface of the PV panel in two different numbers, 54 pcs and 108 pcs, and four different arrangements, 54 pc shifted (type 1), 54 pc staggered (type 2), 108 pc double-shifted (type 1), and 108 pc shifted (type 2). For 54 pc type 1 fins, odd and even rows have 4 and 5 fins, respectively. The vertical spacing between each row is set to be 10.5 cm, with a horizontal spacing of 12.5 cm between fins. In the staggered second arrangement (type 2), each row is staggered one over another with a 5 cm vertical spacing, and spacing between fins is again 12.5 cm. This configuration is a grouped form of type 1, having a vertical spacing of 20 cm between the row groups. As for 108 pc copper fins, in a double-shifted type 1 arrangement, odd and even rows have 8 and 10 fins, respectively. The vertical spacing of each row is 10 cm, and the horizontal spacing between the fins is 5.5 cm. In a shifted type 2 arrangement, odd rows and even rows have 9 and 10 fins, respectively, except for the last two rows missing 3 fins on both sides in order to keep the number of fins the same as in type 1. The vertical spacing between the rows is 5 cm, and the horizontal spacing between fins is 5.5 cm. The amount of radiation was kept constant at $\dot{Q}_{\text{solar}} = 1100\ \text{W/m}^2$ by using artificial solar lamps during the experiments. The intensity of this radiation is the maximum insolation level which can be measured on earth.

As shown in Figure 4, the test setup is mainly composed of two basic sections, namely, the test section and the control section, and 17 parts or auxiliary elements named in Table 2.

The law of conservation of mass (also referred to as the first law), the most basic law of thermodynamics, applies to all thermodynamic calculations. Before performing the thermodynamic analysis of the photovoltaic thermal (PVT) system, which is the subject of this study, it should be noted that the system is a control volume with continuous flow (an open system). A control volume is the general name for systems with a mass flow within their boundaries. Both mass and energy can be transferred through the boundaries of the control volume [21–24].

The mass transfer from any system to the control volume or from the control volume to the system in a Δt time interval is equal to the change of mass in the control volume at that time interval [25, 26].

$$\dot{m}_{\text{inlet}} - \dot{m}_{\text{outlet}} = \Delta_{\text{cv}} \left[\frac{\text{kg}}{\text{s}}\right]. \quad (1)$$

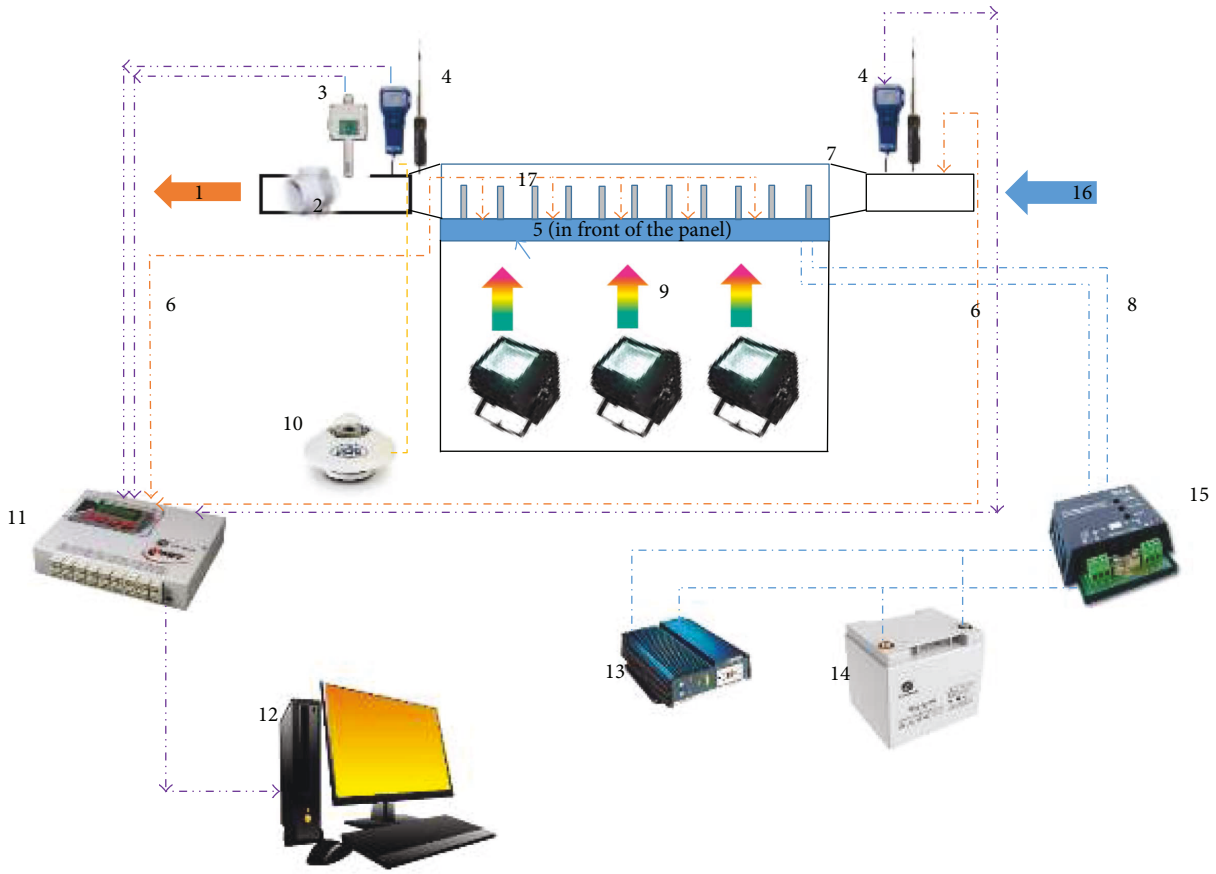

Figure 4: Experimental schematic setup.

Table 2: Parts of the experimental setup.

Test section
(1) Air outlet
(2) Fan
(3) Temperature humidity transmitter
(4) Input velocity anemometer
(5) Photovoltaic panel
(6) Thermocouple
(7) Control volume
(8) Photovoltaic power transmission
(9) Artificial solar radiation
Control section
(10) Pyranometer
(11) Data logger
(12) Computer
(13) DC-AC inverter
(14) Acidic gel battery
(15) Solar charger regulator
(16) Air inlet
(17) Cooling fins

The energy equation for a continuous flow system, as given by Masters [27] and Radziemska [21], is

$$\dot{Q}_U = \dot{m} \cdot c_p (T_{\text{inlet}} - T_{\text{outlet}}) \,[\text{kW}]. \tag{2}$$

The total useful solar power from the sun is the sum of the thermal power gain and the electrical power production ($\dot{Q}_e = I \cdot V$) [28–31] and is given as

$$\dot{Q}_{\text{gain}} = \dot{m}\left[c_p (T_{\text{inlet}} - T_{\text{outlet}})\right] + I \cdot V \,[\text{kW}]. \tag{3}$$

The total electrical energy produced is obtained if the energy drawn by the fan ($W_{\text{fan}} = I_{\text{fan}} \cdot V_{\text{fan}}$) is removed, and the first-law efficiency, as given by Zagorska et al. [29] and Zimmermann et al. [31], is

$$\begin{aligned} \eta_I &= \frac{\dot{Q}_u + \dot{Q}_e - W_{\text{fan}}}{\dot{Q}_{\text{solar}}} \\ &= \frac{\dot{Q}_{\text{gain}} - W_{\text{fan}}}{\dot{Q}_{\text{solar}}}. \end{aligned} \tag{4}$$

When there is a flow in the system, regarding the calculations, it is important to determine whether the flow is

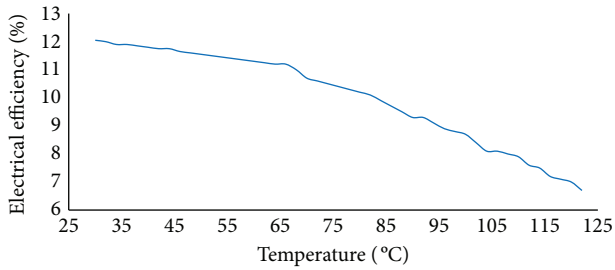

Figure 5: Electrical efficiency-temperature of the noncooling panel.

compressible or incompressible. Whether the compressibility effect in a flow is important or not is concluded by calculating the Mach number. If the Mach number is less than 0.3, the flow is considered incompressible.

$$\mathrm{Ma} = \frac{V}{c}, \tag{5}$$

where c is the speed of sound ($c = 340.29$ m/s) and V is the velocity of the fluid, whereby the flow is concluded to be Newtonian.

$$Q = h \cdot A_{\mathrm{pv}} \cdot \left(\Delta T_{\mathrm{air}} - T_{\mathrm{pv}}\right) [\mathrm{kW}]. \tag{6}$$

Using (6), with the help of the energy the air has gained within the designed control volume, the total heat transfer coefficient for the system can be calculated. As the total heat transfer coefficient is a function of the total heat drawn from the system, Nusselt number calculation can be made there from

$$\mathrm{Nu} = \frac{h \cdot D_{\mathrm{h}}}{k_{\mathrm{air}}}. \tag{7}$$

Against each Reynolds value for the air acting as the refrigerant in the system, a different Nusselt number will correspond.

The channel friction factor can be computed along the test section by pressure loss, ΔP, as

$$f = \frac{\Delta P}{(L/D_{\mathrm{h}}) \cdot \rho \cdot U_{\mathrm{m}}^2/2}. \tag{8}$$

In this equation, ρ is density of film temperature of the air and U_{m} is the average velocity of the fluid.

In the subject of strategies for heat transfer enhancement, enough attention should be paid towards flow resistance, friction factor value, and performance factor.

Regarding the Nu number and friction factor, the performance factor of the fins is evaluated to have an appropriate comparison of overall thermohydrodynamic performance among test fins. Performance evaluation criteria, η, is written as [32–34]

$$\eta = \left(\frac{\mathrm{Nu}}{\mathrm{Nu}_0}\right)\left(\frac{f_0}{f}\right)^{1/3}, \tag{9}$$

where f_0 and Nu_0 are the friction factor and Nusselt number of the plain channel, respectively.

With the aim of validation, the obtained Nusselt number (Nu) and friction factor (f) of the plain channel have been compared to those correlations proposed in the literature. The empirical correlations for the plain channel are considered to achieve the Nusselt number and friction factor as [35, 36]

$$\begin{aligned}
&\mathrm{Nu} = 0.023\mathrm{Re}^{0.8}\,\mathrm{Pr}^{\frac{1}{3}}\text{: Colburn correlation } \left(\text{for } 10^4 \le \mathrm{Re}\right),\\
&\mathrm{Nu} = 0.023\mathrm{Re}^{0,8}\,\mathrm{Pr}^{n}\ (n = 0.3\text{–}0.4)\text{: Dittus-Boelter correlation } \left(\text{for } 10^4 \le \mathrm{Re}\right),\\
&f = 0.316\mathrm{Re}^{-0.25}\text{: Blasius correlation } \left(\mathrm{Re} \le 20000\right),\\
&f = \left(0.790\ln \mathrm{Re} - 1.64\right)^{-2}\text{: Petukhov correlation } \left(\text{for } 3000 \le \mathrm{Re} \le 5 \times 10^6\right).
\end{aligned} \tag{10}$$

To compare the experimental results, experiments were performed using the identical fins in different numbers and arrangements as shown in Figure 3.

3. Results and Discussion

The surface temperature of a noncooled photovoltaic panel increased to about 120°C over time due to the fact that solar cells convert only a small portion of incident solar radiation into electricity and accumulates the rest as waste heat in the unit unless it is recovered and utilized through another thermal system [37]. The ratio of generated electrical energy to total incoming energy is called the electrical efficiency, whereas the thermal efficiency is the ratio of net utilized thermal energy to total incident solar energy received on the PV panel.

The increase in cell temperature reduces the electrical efficiency of the photovoltaic panel, which is plotted versus the surface temperature in Figure 5.

In order to keep the electrical efficiency of the photovoltaic panel at an appropriate level, the optimum cell temperature should be around 50–60 degrees. In order to achieve the necessary cooling in the cell temperature, the heat transfer surface area was increased using fins, convection heat transfer was increased using forced circulation, and different fin arrangements were tried in order to create turbulence within the air flow.

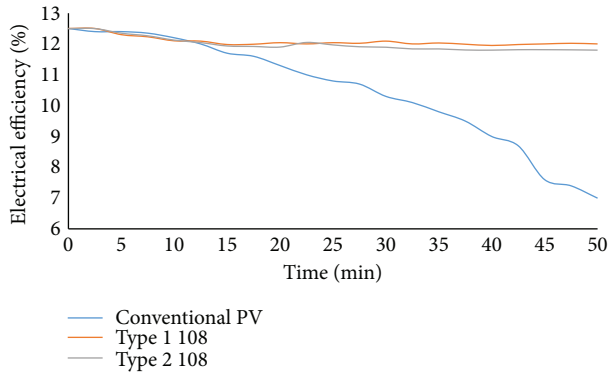

Figure 6: Change of electrical efficiency with 108 pc fin arrangements at 4.5 m/s.

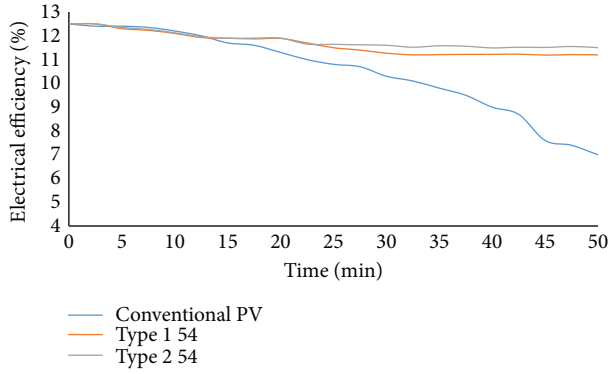

Figure 7: Change of electrical efficiency with 54 pc fin arrangements at 4.5 m/s.

Consequently, the total heat drawn from the PV panel has been increased and the cell temperature decreased to near optimum operating temperature; hence, the electrical efficiency could be maintained at higher levels.

The improvement in the electrical efficiency of the photovoltaic panel is shown in Figures 6 and 7 per fin arrangement at 4.5 m/s. In the experiments, it was observed that electrical efficiency did not change during the first 15-minute time period, but electrical efficiency decreased drastically in the next time period. As a result, while the electrical efficiency of the uncooled photovoltaic panel reduced from 12.5% to approximately 7%, thanks to the heat transfer enhancement provided by 54 pc fin arrangements and 108 pc fin arrangements used in active cooling, the reduction in the electrical efficiency has been prevented at a significant extent and could be kept at fairly high levels. Efficiencies for type 1 and type 2 arrangements of 108 pc fins are 12.02% and 11.81%, respectively (Figure 6). As for 54 pc fin type 1 and type 2 arrangements, these figures were 11.2% and 11.55%, respectively (Figure 7).

The rate of change in the thermal efficiency of the PV/T panel is shown in Figures 8 and 9 for different arrangements. The best thermal efficiency rate increased to 74% at type 108 and to 60% at type 54. The improvement of thermal efficiency increased the electrical efficiency as well.

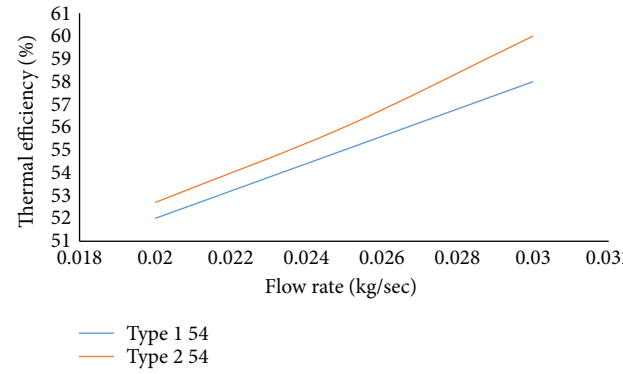

Figure 8: Variation of thermal efficiency versus flow rate (kg/s) for 54 pc arrangements.

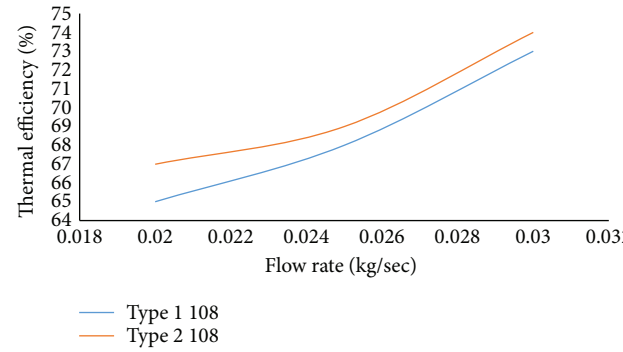

Figure 9: Variation of thermal efficiency versus flow rate (kg/s) for 108 pc arrangements.

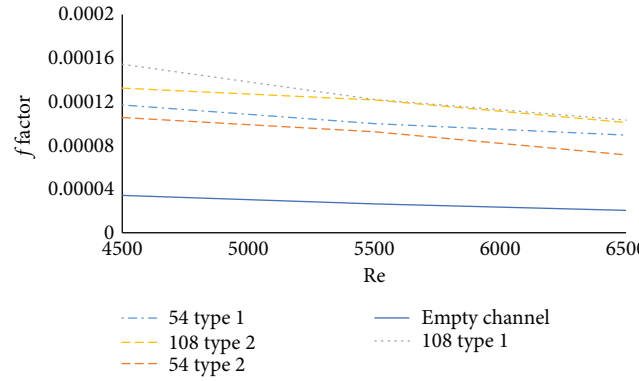

Figure 10: Friction factor—Reynolds number.

The heat transfer friction factor and heat transfer coefficient of fins used in the experiments are given in Figures 10 and 11. As seen from Figures 10 and 11, while the rate of heat transfer increased with increasing air velocity, the effectiveness of the friction coefficient decreased.

Figure 12 shows the change in Reynolds number and thermal enhancement factor (η) for all fin arrangements. Nusselt number and friction factor values were compared for the same Reynolds number. It is seen that all thermal enhancement factor values are above 1. With increased Reynolds numbers, there is generally a decrease in the

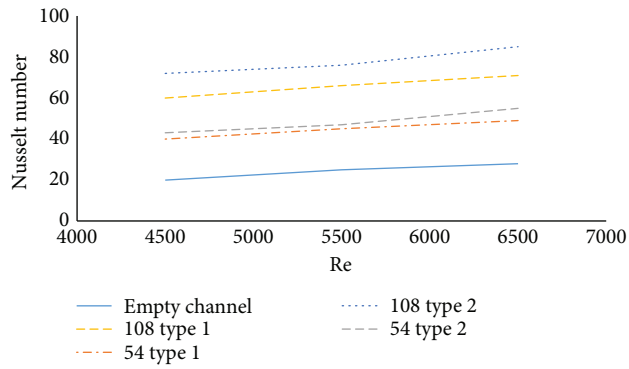

Figure 11: Nusselt representations of different fin configurations in the photovoltaic system.

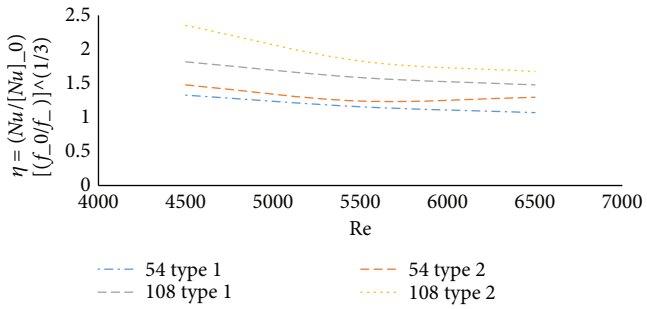

Figure 12: Thermal enhancement factor η for varying Reynolds numbers.

thermal enhancement factor. The best result for the thermal enhancement factor was 108 type 2, while 54 type 1 gave the lowest result.

In order to validate these results obtained from the experiments, a CFD model was prepared. The boundary conditions used for the CFD analysis were chosen to be those in effect in the experimental evaluation, wherein the input air temperature is 23°C, the solar irradiance is 1100 W/m^2, and air velocities are 3.3, 3.9, and 4.5 m/s. In the model preparation, the most important phase prior to the solution is the phase in which the material properties are defined, the geometric model is established, and meshing is performed.

A solution validation study was performed according to the CFD verification and validation standard to evaluate the mesh uncertainty and appropriate mesh parameters for the mesh simulation.

For the model presented in Figure 13, nonstructural four-sided cages were formed which were refined with prismatic near-wall elements (inflated). Stage grating treatments with a factor of 1.3 were applied to the edge separation bar and bar. The ratio between the height of the last six-sided layer and the first prism was the same for all cages. Also, different manifold designs were modeled using the ANSYS Fluent program, the CFD of generic calculated fluids, to provide for the distribution of flows in channels.

The standard k-ε model solution does not require a wall model for the solution of the problem. In the k-ε turbulence models, "enhanced wall function" was used as the wall model. The enhanced wall function is the most advanced mode among the wall models. This model also incorporates the viscous effects in the walls to provide a more appropriate solution to the problem.

In addition, by forming a boundary layer effect on the hulls, it was seen that the flow structure gave better results in this study. The transfer equations, the method of calculating the turbulence viscosity, and the model constants are different for each model. The generation of turbulence, turbulence due to the lift force, the calculation of the effects of compressibility, and the modeling of heat and mass transfer are essentially common within each model.

In Figures 14–16 are images obtained from the simulations showing velocity contours for three different air velocities per configuration, along with those for the empty control volume. It can easily be seen from these figures that, with the contribution of forced air circulation, dead volume zones, where there is no or very low flow circulation occurs, have been significantly removed, especially in the air outlet region.

As it is seen in Figure 16, the air flow distribution throughout the cross section of the control volume is more intense and temperature distribution is more homogeneous. Moreover, it may be concluded that the air circulation is more effective due to the turbulent air flows in the vicinity of fins. The simulation results also suggest that all fin arrangements, in terms of providing uniform flow distribution with no recirculation, are efficient.

No doubt, the designed system will help draw more heat from the PV module and reduce the temperature during operation, which in turn will help maintain the electrical efficiency at higher levels. But the point is whether another satisfactory configuration with less fins and lower air velocity is possible with just changing the fin arrangement or not. Temperature contours suggest that it is.

Figures 17–19 show the temperature distribution for three different air velocities in all configuration types. As seen in Figures 17–19, the blown air could draw almost no heat from the panel surface at any air velocities when the control volume has no fins installed within. Again, for this configuration, the intensity of dead volume where the air gets stuck and heated up is significant. For 54-piece and 108-piece type 1 arrangements, the temperature distribution is far better, and the removal of dead volume is clearly seen in Figures 17–19.

The best temperature distribution, hence the most heat drawing as well as minimum dead volume zones, is achieved with a 108-piece type 2 arrangement at 4.5 m/s air velocity, which is quite foreseeable, but the most important finding here is that the resulting 54-piece fins in type 1 arrangement offers is very close to those of 108-piece type 1 and type 2. This shows that the arrangement is as much important a parameter as the heat transfer surface area for the total heat transfer rate. Taking into account the cost of fins and the friction loss, and the pressure drop, hence the increased fan power, the 54-piece type 1 arrangement can be preferred rather than any arrangement of 108-piece fins.

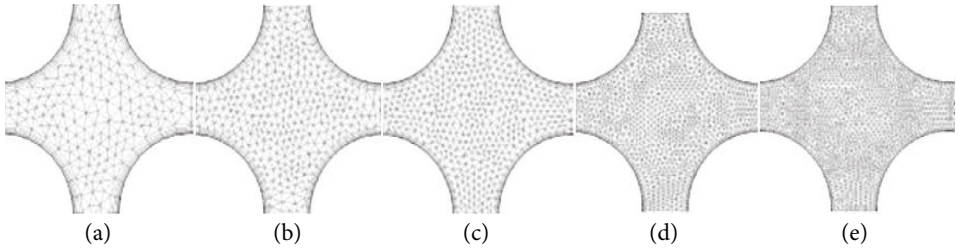

Figure 13: Mesh section in the areas where there are no fins.

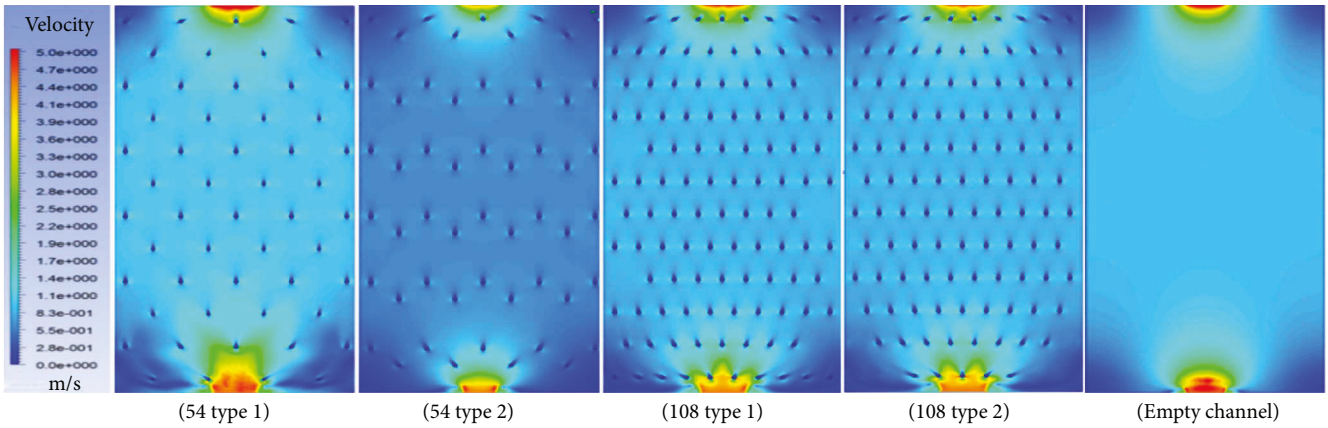

Figure 14: Velocity contours at 4.5 m/s.

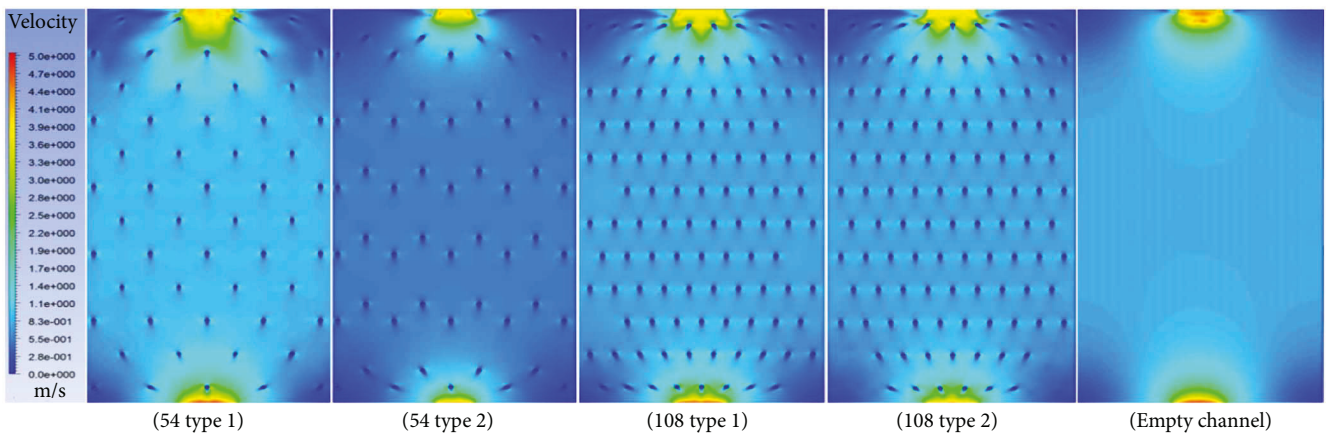

Figure 15: Velocity contours at 3.9 m/s.

4. Conclusion

In this work, both electrical and thermal energy is produced by the hybrid PV/T system. The electrical efficiencies of the PV/T panels are severely reduced as the surface temperatures increase. Cooling the surface of the panel is an effective way to avoid this reduction in efficiency. If no cooling is used, the operating temperature of the PV module reaches a value as high as 120°C and the electrical efficiency drops about to 7% from 12.5%. As the efficiency of the PV panel without active cooling decreases in relation to increasing surface temperature when the panel is not cooled, the forced convection heat transfer zone is formed in the control volume in the back of the PV panel. As a result, a cooling of up to 60–65 degrees at the surface temperature of 120 degrees has been achieved, so the decrease in the electrical current is prevented to a great extent and the efficiency could be maintained at 12.02%.

Consequent turbulent air flows occurring within the control volume, especially in the vicinity of the fins, contributes to heat removal from the panel; therefore, with the 108 pc type 1 arrangement, the highest efficiency was achieved

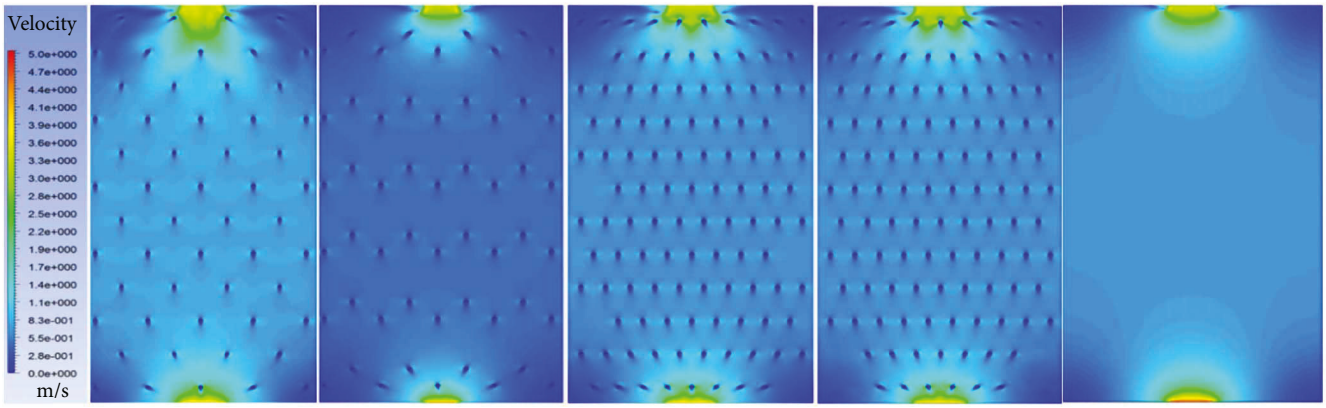

Figure 16: Velocity contours at 3.3 m/s.

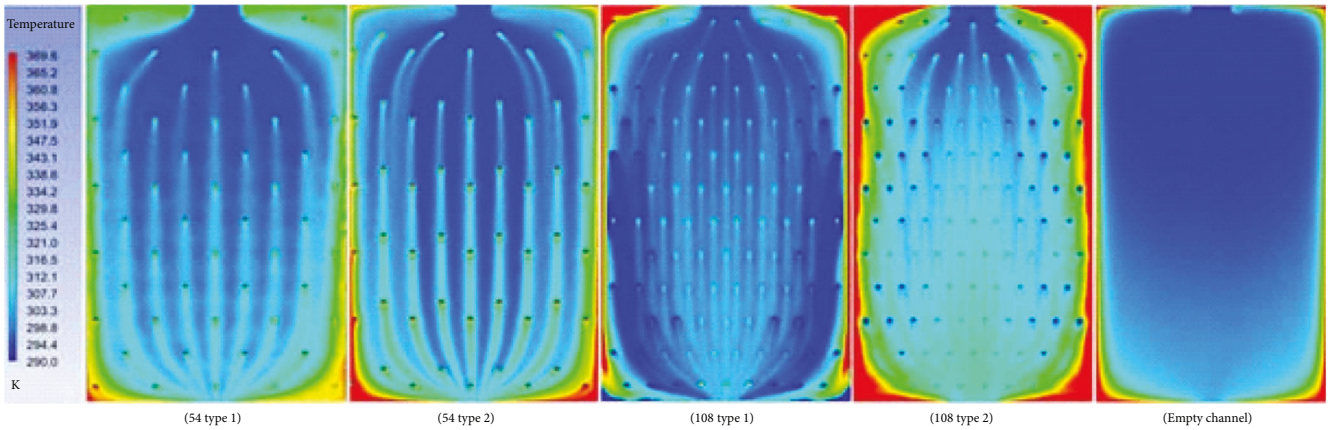

Figure 17: Temperature contours at 4.5 m/s.

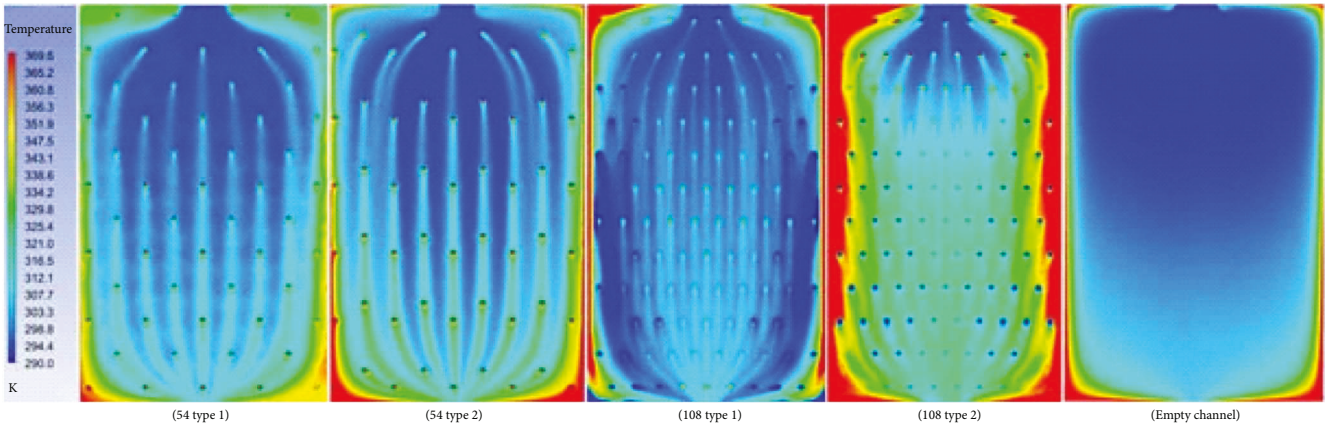

Figure 18: Temperature contours at 3.9 m/s.

at 12.02% as expected. Nevertheless, while the 108 pc type 2 arrangement could maintain the electrical efficiency at 11.81%, a close level of 11.55% could be obtained with the 54 pc type 2 arrangement, whereby we can see the impact of arrangement on heat transfer and could conclude that there is a threshold value for the heat transfer surface area somewhere between 50 and 60 pc fins. Similar efficiency gains can be achieved by using fewer fin elements and by

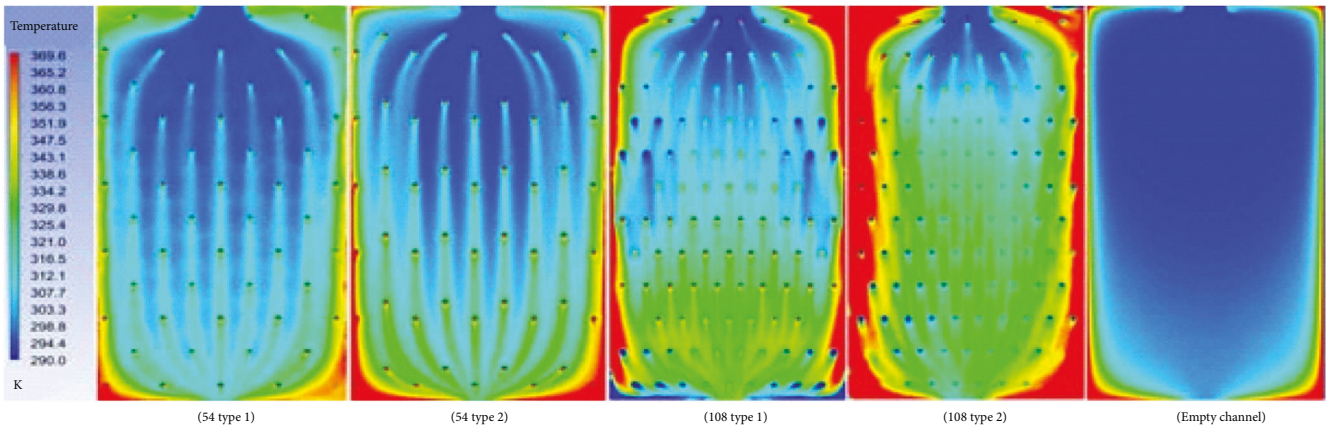

Figure 19: Temperature contours at 3.3 m/s.

creating the correct turbulence model compared to the cost of the cooling unit.

The best panel efficiency was with 108-piece type 1 at 4.5 m/s air velocity, but the efficiency achieved with the 54-piece type 2 arrangement was very close with 11.55%. This suggests that, thanks to the turbulence effect created by the fin arrangement, the heat transfer rate with 54 fins has been very close to that of twice as much fins.

In addition to the heat transfer surface area and air velocity, it is seen that the fin arrangement is an important parameter in the heat transfer rate. It can be concluded that with better designed fin arrangements, the required fan speed could be lowered for any number of fins or similar results could be obtained with fewer fins. On the other hand, since the power required by the PV-powered fan will also decrease with fewer fins and at lower air velocities, the total efficiency obtained from the PV system will also increase.

Nomenclature

c: Velocity of sound (m/s)
$\dot{Q}_e$: Electrical power production (W)
$\dot{Q}_u$: Usable thermal power (W)
$\dot{Q}_{solar}$: Solar radiation (W/m^2)
$\Delta\dot{m}_{cv}$: Difference of mass in control volume (kg/s)
Ma: Mach number
$\dot{m}_{inlet}$: Inlet mass of air (kg/s)
$\dot{m}_{outlet}$: Outlet mass of air (kg/s)
I: Direct current (A)
V: Voltage (volts)
η: Performance evaluation criteria
ρ: Density of film temperature of the air
U_m: Average fluid velocity
Re: Reynolds number
Nu: Nusselt number
Pr: Prandtl number
T_{inlet}: Inlet air temperature (°C)
T_{outlet}: Outlet air temperature (°C)
v: Velocity of air (m/s)
w_{fan}: Work of fan (W)
c_p: Specific heat capacity (J/kg·K)
h: Heat transfer coefficient in air duct (W/m^2·K)
A_{pv}: Aperture area of PV module (m^2)
T_{air}: Air temperature (°C)
T_{pv}: Photovoltaic cell temperature (°C)
Nu: Nusselt number
$\dot{Q}_{gain}$: Gained total power (W)
k: Heat transfer coefficient for conduction (W/m·K)
f: Friction factor
Dh: Effective diameter of the channel
ΔP: Pressure loss
L: Channel length.

Conflicts of Interest

The author declares that he has no conflicts of interest.

Acknowledgments

The author would like to thank the laboratory staff of Atatürk University Engineering Faculty Mechanical Engineering for their time and support.

References

[1] A. Fudholi, K. Sopian, M. H. Ruslan, M. A. Alghoul, and M. Y. Sulaiman, "Review of solar dryers for agricultural and marine products," *Renewable and Sustainable Energy Reviews*, vol. 14, no. 1, pp. 1–30, 2010.

[2] M. Grupp, H. Bergler, J. P. Bertrand, B. Kromer, and J. Cieslok, ""Convective" flat plate collectors and their applications," *Solar Energy*, vol. 55, no. 3, pp. 195–207, 1995.

[3] O. Ekechukwu and B. Norton, "Review of solar-energy drying systems III: low temperature air-heating solar collectors for crop drying applications," *Energy Conversion and Management*, vol. 40, no. 6, pp. 657–667, 1999.

[4] H. A. Zondag, W. G. J. Van Helden, M. Bakker et al., *PVT roadmap. A European guide for the development and market introduction of PVT Technology*, Energy research Centre of the Netherlands ECN, Petten (Netherlands), 2006.

[5] N. Wijeysundera, L. L. Ah, and L. E. Tjioe, "Thermal performance study of two-pass solar air heaters," *Solar Energy*, vol. 28, no. 5, pp. 363–370, 1982.

[6] C. Choudhury, P. Chauhan, and H. Garg, "Performance and cost analysis of two-pass solar air heaters," *Heat Recovery Systems and CHP*, vol. 15, no. 8, pp. 755–773, 1995.

[7] A. Joshi, A. Tiwari, G. N. Tiwari, I. Dincer, and B. V. Reddy, "Performance evaluation of a hybrid photovoltaic thermal (PV/T) (glass-to-glass) system," *International Journal of Thermal Sciences*, vol. 48, no. 1, pp. 154–164, 2009.

[8] C. Choudhury, P. M. Chauhan, H. P. Garg, and S. N. Garg, "Cost—benefit ratio of triple pass solar air heaters," *Energy Conversion and Management*, vol. 37, no. 1, pp. 95–116, 1996.

[9] C. Ho, C. Yeh, and S. Hsieh, "Improvement in device performance of multi-pass flat-plate solar air heaters with external recycle," *Renewable Energy*, vol. 30, no. 10, pp. 1601–1621, 2005.

[10] A. Fudholi, M. Ruslan, and K. Sopian, "Review of multi-pass solar air collectors with heat transfer surface enhancement," in *Proceedings of the 4th Scientific Conference PPI-UKM*, pp. 3–11, Supranto, Malaysia, 2009.

[11] A. Fudholi, K. Sopian, M. Y. Othman et al., *Heat transfer correlation for the V-groove solar collector*, Solar Energy Research Institute, University Kebangsaan Malaysia, 43600 Bangi Selangor Malaysia, 2008.

[12] M. Hafiz, M. Y. Othman, M. M. Salleh, and K. Sopian, "Design and indoor testing of the V-groove back pass solar collector," *Renewable Energy*, vol. 16, pp. 2118–2122, 1999.

[13] W. Gao, W. Lin, T. Liu, and C. Xia, "Analytical and experimental studies on the thermal performance of cross-corrugated and flat-plate solar air heaters," *Applied Energy*, vol. 84, no. 4, pp. 425–441, 2007.

[14] A. Kolb, E. Winter, and R. Viskanta, "Experimental studies on a solar air collector with metal matrix absorber," *Solar Energy*, vol. 65, no. 2, pp. 91–98, 1999.

[15] A. Abdullah, H. Abou-Ziyan, and A. Ghoneim, "Thermal performance of flat plate solar collector using various arrangements of compound honeycomb," *Energy Conversion and Management*, vol. 44, no. 19, pp. 3093–3112, 2003.

[16] K. Matrawy, "Theoretical analysis for an air heater with a box-type absorber," *Solar Energy*, vol. 63, no. 3, pp. 191–198, 1998.

[17] K. Sopian, M. A. Alghoul, E. M. Alfegi, M. Y. Sulaiman, and E. A. Musa, "Evaluation of thermal efficiency of double-pass solar collector with porous–nonporous media," *Renewable Energy*, vol. 34, no. 3, pp. 640–645, 2009.

[18] S. Youcef-Ali, "Study and optimization of the thermal performances of the offset rectangular plate fin absorber plates, with various glazing," *Renewable Energy*, vol. 30, no. 2, pp. 271–280, 2005.

[19] M. A. Karim and M. Hawlader, "Performance investigation of flat plate, v-corrugated and finned air collectors," *Energy*, vol. 31, no. 4, pp. 452–470, 2006.

[20] P. Naphon, "On the performance and entropy generation of the double-pass solar air heater with longitudinal fins," *Renewable Energy*, vol. 30, no. 9, pp. 1345–1357, 2005.

[21] E. Radziemska, "The effect of temperature on the power drop in crystalline silicon solar cells," *Renewable Energy*, vol. 28, no. 1, pp. 1–12, 2003.

[22] M. Rahman, M. Hasanuzzaman, and N. Rahim, "Effects of various parameters on PV-module power and efficiency," *Energy Conversion and Management*, vol. 103, pp. 348–358, 2015.

[23] E. Saloux, A. Teyssedou, and M. Sorin, "Analysis of photovoltaic (PV) and photovoltaic/thermal (PV/T) systems using the exergy method," *Energy and Buildings*, vol. 67, pp. 275–285, 2013.

[24] F. Sobhnamayan, F. Sarhaddi, M. A. Alavi, S. Farahat, and J. Yazdanpanahi, "Optimization of a solar photovoltaic thermal (PV/T) water collector based on exergy concept," *Renewable Energy*, vol. 68, pp. 356–365, 2014.

[25] H. Teo, P. Lee, and M. Hawlader, "An active cooling system for photovoltaic modules," *Applied Energy*, vol. 90, no. 1, pp. 309–315, 2012.

[26] J. Tonui and Y. Tripanagnostopoulos, "Air-cooled PV/T solar collectors with low cost performance improvements," *Solar Energy*, vol. 81, no. 4, pp. 498–511, 2007.

[27] G. M. Masters, "Wind power systems," in *Renewable and Efficient Electric Power Systems*, pp. 307–383, John Wiley & Sons, Inc., Hoboken, NJ, USA, 2005.

[28] J. Tonui and Y. Tripanagnostopoulos, "Performance improvement of PV/T solar collectors with natural air flow operation," *Solar Energy*, vol. 82, no. 1, pp. 1–12, 2008.

[29] V. Zagorska, I. Ziemelis, L. Kancevica, and H. Putans, "Experimental investigation of photovoltaic-thermal hybrid solar collector," *Agronomy Research Biosystem Engineering Special*, vol. 1, pp. 227–234, 2012.

[30] W. Harry, *Recent facts about photovoltaics in Germany*, Fraunhofer Institute for Solar Energy Systems (ISE), Germany, 2014.

[31] S. Zimmermann, H. Helmers, M. K. Tiwari et al., "A high-efficiency hybrid high-concentration photovoltaic system," *International Journal of Heat and Mass Transfer*, vol. 89, pp. 514–521, 2015.

[32] P. Promvonge, "Thermal augmentation in circular tube with twisted tape and wire coil turbulators," *Energy Conversion and Management*, vol. 49, no. 11, pp. 2949–2955, 2008.

[33] S. Eiamsa-ard and P. Promvonge, "Experimental investigation of heat transfer and friction characteristics in a circular tube fitted with V-nozzle turbulators," *International Communications in Heat and Mass Transfer*, vol. 33, no. 5, pp. 591–600, 2006.

[34] G. Ömeroğlu, "Experimental and computational fluid dynamics analysis of a photovoltaic/thermal system with active cooling using aluminum fins," *Journal of Photonics for Energy*, vol. 7, no. 4, article 045503, 2017.

[35] K. Yakut and B. Sahin, "The effects of vortex characteristics on performance of coiled wire turbulators used for heat transfer augmentation," *Applied Thermal Engineering*, vol. 24, no. 16, pp. 2427–2438, 2004.

[36] S. Eiamsa-ard and P. Promvonge, "Enhancement of heat transfer in a tube with regularly-spaced helical tape swirl generators," *Solar Energy*, vol. 78, no. 4, pp. 483–494, 2005.

[37] Ö. İlhan Volkan, M. K. Yeşilyurt, E. Ç. Yilmaz, and G. Ömeroğlu, "Photovoltaic thermal (PVT) solar panels," *International Journal of New Technology and Research*, vol. 2, no. 12, pp. 13–16, 2016.